FULL PAPER

Liquid-Crystalline Electrolytes for Lithium-Ion Batteries: Ordered Assemblies of a Mesogen-Containing Carbonate and a Lithium Salt

*Junji Sakuda, Eiji Hosono, Masafumi Yoshio, Takahiro Ichikawa, Takuro Matsumoto, Hiroyuki Ohno, Haoshen Zhou, and Takashi Kato**

Thermotropic liquid-crystalline (LC) electrolytes for lithium-ion batteries are developed for the first time. A rod-like LC molecule having a cyclic carbonate moiety is used to form self-assembled two-dimensional ion-conductive pathways with lithium salts. Electrochemical and thermal stability, and efficient ionic conduction is achieved for the liquid crystal. The mixture of the carbonate derivative and lithium *bis*(trifluoromethylsulfonyl)imide is successfully applied as an electrolyte in lithium-ion batteries. Reversible charge–discharge for both positive and negative electrodes is observed for the lithium-ion batteries composed of the LC electrolyte.

1. Introduction

Functional liquid crystals have attracted much attention as transport materials of charges and ions.[1,2] Development of new ion-transport materials is important for the improvement of energy devices. A variety of electrolytes, such as gel electrolytes,[3a,b] ionic plastic crystals,[3c-e] polymer electrolytes,[3f-h] inorganic solid electrolytes,[4] and nanostructured liquid crystals[2] have been proposed. Among them, ion-conductive nanostructured liquid crystals have great potential as new electrolytes because they provide efficient 1D,[5] 2D,[6] and 3D[2a,7] ion-conductive pathways. These organized pathways having regular pore sizes[8] are expected to contribute to the efficient transport of ions. In particular, lithium-,[2a,5,6a-d,7a,c] proton-,[9] and iodides-[10] transport materials are of interest due to their potential application as electrolytes in lithium-ion batteries, fuel cells, and dye-sensitized solar cells, respectively. Our intention here is to use liquid-crystalline (LC) electrolytes in lithium-ion batteries.[11] Organic liquid[12] and gel[3a,b] electrolytes are currently used in commercial lithium-ion batteries. These electrolytes inherently have risks of leakage, evaporation, and flammability. To overcome these issues, nonvolatile electrolytes with high ionic conductivities are needed. Inorganic solid electrolytes such as $Li_{10}GeP_2S_{12}$[4a] are one of the promising candidates. However, a majority of inorganic solid electrolytes suffer from low ionic conductivities and the difficulties in processability and in interfacial compatibility of the electrolytes with electrode materials.[4] In this context, we considered that nanostructured liquid crystals can be used as new electrolytes because of their potential to form ion-conductive pathways with liquid-like mobility.[2b] If we polymerize reactive liquid crystals keeping nanoscale mobile channels, we could have nonvolatile efficient conductors.[2b,6b,13] Moreover, to obtain LC materials for the batteries, we need materials having continuous channels that show efficient transport of lithium ions between the electrodes. It is also important that the nanostructured electrolytes are electrochemically stable in the high voltage systems of lithium-ion batteries. To our knowledge, there is no report on thermotropic LC electrolytes for lithium-ion batteries. Herein, we report nanostructured LC materials which are applied as electrolytes in lithium-ion batteries. Reversible charge–discharge of both positive and negative electrode materials has been successfully achieved.

In order to obtain efficient and stable thermotropic LC electrolytes, we focused on carbonate-based liquid crystals. Carbonate derivatives are practically used in lithium-ion batteries because of their high dielectric constants for the dissociation of lithium salts and sufficient electrochemical stability.[12] Gel electrolytes containing carbonates have been reported in the course of development of solid electrolytes.[3a,b] Previously, we reported a fan-shaped molecule having a cyclic carbonate moiety that forms columnar LC structures when mixed with lithium salts. However, this carbonate-derived columnar liquid crystal showed low ionic conductivities in the order of 10^{-8} S cm^{-1}.[5a] In the present study, layered LC structures have been employed as ion-conductive media for batteries because ion-conductive smectic

J. Sakuda, Dr. M. Yoshio, Prof. T. Kato
Department of Chemistry and Biotechnology
School of Engineering
The University of Tokyo
Hongo, Bunkyo-ku, Tokyo 113-8656, Japan
E-mail: kato@chiral.t.u-tokyo.ac.jp
Dr. E. Hosono, Dr. H. Zhou
Energy Technology Research Institute
National Institute of Advanced Industrial Science and Technology
Umezono, Tsukuba, Ibaraki 305-8568, Japan
Dr. T. Ichikawa, T. Matsumoto, Prof. H. Ohno
Department of Biotechnology
Tokyo University of Agriculture and Technology
Nakacho, Koganei, Tokyo 184-8588, Japan

DOI: 10.1002/adfm.201402509

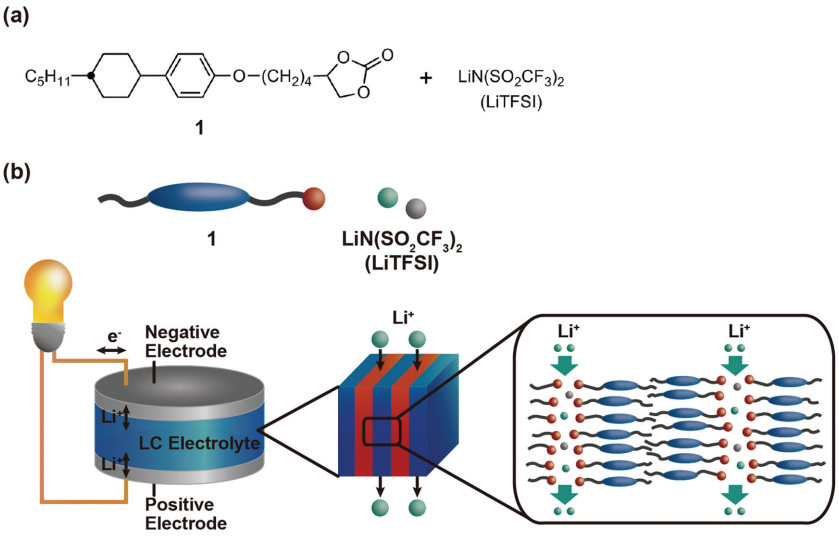

Figure 1. a) Molecular structures of compound **1** and the lithium salt. b) Schematic illustration of our concept and design for the lithium-ion battery containing the LC electrolyte.

liquid crystals form wide and highly mobile 2D ion-conductive pathways,[6] although 1D and 3D ionic channels based on nanostructured liquid crystals can be used.[2b] Our intention here is that we show potential of nanostructured smectic liquid crystals for lithium-ion batteries because the area of 2D conductive pathways seems to be larger than those of 1D and 3D. We have designed and synthesized rod-like molecule **1** having a mesogenic unit and a cyclic carbonate moiety at the terminal of the alkyl chain (**Figure 1**a). We expected that the mixtures of compound **1** and lithium *bis*(trifluoromethylsulfonyl)imide (LiTFSI) form 2D ion-conductive pathways through ion–dipole interactions between cyclic carbonate groups and lithium ions (Figure 1b). A cyclohexylphenyl group has been introduced as the rigid-rod mesogenic moiety because it is assumed that the mesogenic part is relatively electrochemically stable.

2. Results and Discussion

2.1. Liquid-Crystalline Properties

Self-assembled electrolytes consisting of compound **1** and LiTFSI were obtained by evaporation of the solvent from tetrahydrofuran solutions of **1** and LiTFSI. Compound **1** and LiTFSI are miscible up to a mole fraction of 0.4 for LiTFSI. **Figure 2**a shows a phase diagram of the mixtures of compound **1** and LiTFSI. Compound **1** alone shows a smectic A (SmA) phase ranging from 96 to 22 °C and a subsequent smectic B (SmB) phase on cooling (Supporting Information, Figures S1–S3). The mixtures exhibit SmA phases in wide temperature ranges. The isotropization temperatures increase when **1** is mixed with LiTFSI at the mole fractions of up to 0.25 (Figure 2a). This observation suggests that ion–dipole interactions between lithium ions and the cyclic carbonate groups of **1** stabilize the nanosegregated layered structures in the SmA phases. Further addition of LiTFSI results in a decrease in the isotropization temperatures. The incorporation of large TFSI anions may destabilize the LC structures. The SmA–SmB phase transition temperatures decrease by the increase in the amount of LiTFSI and no SmB phase is seen for the mixtures containing more than 0.125 mole fraction of LiTFSI. These results are attributed to the fact that the in-plane packing of mesogens within the smectic layer is disturbed by the organization of bulky LiTFSI salts through interactions with the carbonate moieties. Since the molecular motion in a SmA phase is higher than that in a SmB phase,[14] the higher ionic conductivity is expected for the SmA phase.[15] Thus, the electrolyte materials showing the SmA phase in wide temperature ranges seem to be preferable for use in lithium-ion batteries. The mixtures do not crystallize on cooling to −50 °C. The X-ray diffraction pattern of the mixture in the 9:1 molar ratio (Figure 2b) suggests the formation of a lamellar structure with the *d*-spacing of ca. 47 Å. This value is twice the molecular length of **1** estimated to be 22 Å by a molecular mechanics calculation (Merck Molecular Force Field). These results show that the bilayer structures having 2D ion-conductive pathways are formed for the LC electrolyte (Figure 1b).

2.2. Ionic Conductivities

Ionic conductivities of the LC electrolytes were measured by the alternating current impedance method[5b] using comb-shaped gold electrodes deposited on a glass substrate. **Figure 3** shows the ionic conductivities of the mixtures of **1** and LiTFSI on cooling from the isotropic (Iso) states. In the SmA phases, compound **1** shows homeotropic alignment, indicating the formation of 2D ion-conductive pathways parallel to the surface of substrate. Ionic conductivities in the order of 10^{-6}–10^{-4} S cm^{-1} were obtained in the SmA phases. These smectic electrolytes showed higher ionic conductivities than the carbonate-based columnar liquid crystal[5a] exhibiting conductivities around 10^{-8} S cm^{-1}. These results are probably caused by the lower viscosity and the larger area of conduction pathways of the SmA phases. The lithium ions organized into the 1D nanospaces of columnar structures through the coordination of carbonate groups could be transported only along the column axes. On the contrary, the 2D arrays of carbonate groups could allow the transport of lithium ions within the layers along the directions not only parallel but also perpendicular and incline to the applied electric field. In Figure 3, the increase in conductivity at the Iso–SmA phase transitions shown by dot lines was observed because of the formation of the oriented ion-conductive pathways between electrodes. This observation suggests the potential of the LC electrolytes for efficient transport of lithium ions compared to the isotropic liquid crystals. The mixture of **1** and LiTFSI in the 9:1 molar ratio exhibited the highest ionic conductivities among the mixtures. Thus, this mixture was selected as the LC electrolyte for electrochemical measurements.

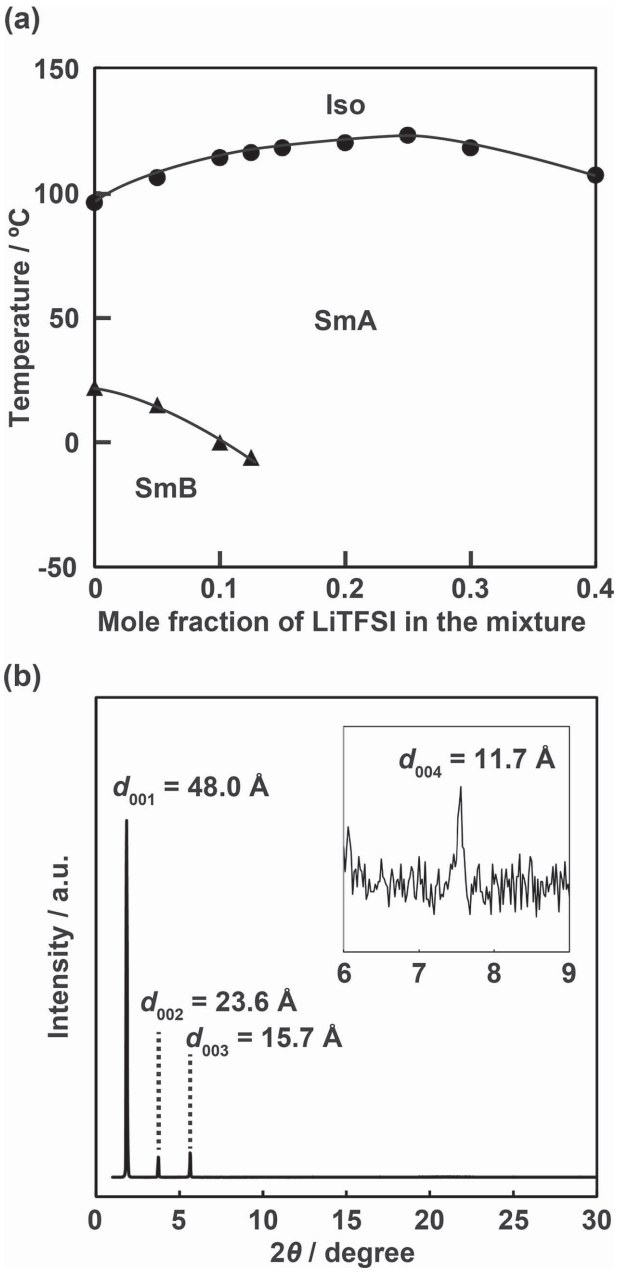

Figure 2. a) Phase transition behavior of the mixtures of **1** and LiTFSI on cooling. Iso: isotropic; SmA: smectic A; SmB: smectic B. b) X-ray diffraction pattern of the mixture of **1** and LiTFSI in the 9:1 molar ratio at 30 °C in the SmA phase.

2.3. Electrochemical Stability

The electrochemical stability of the LC electrolyte was evaluated by cyclic voltammetry on a stainless-steel electrode (SUS316L) using a lithium metal plate as counter and reference electrodes. The measurement was conducted at 60 °C, where the electrolyte exhibits the SmA phase (Figure 2a). The voltammogram at the scan rate of 0.025 mV s^{-1} and in the potential range from –0.5 to 3.9 V versus Li/Li^+ is shown in **Figure 4**. The cathodic

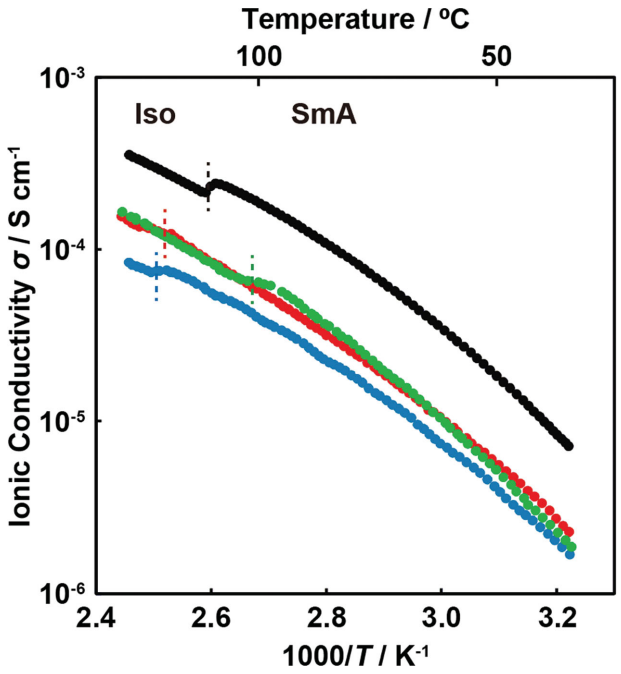

Figure 3. Ionic conductivities of the mixtures of **1** and LiTFSI in the 9:1 (black), 8:2 (blue), 7:3 (red), and 6:4 (green) molar ratios.

and anodic currents corresponding to lithium deposition and dissolution are observed around 0 V versus Li/Li^+. No significant decomposition of the electrolyte is observed in the high potential range over 2 V versus Li/Li^+. The small current below 1.5 V versus Li/Li^+ indicates gradual reduction of **1**. These results suggest that the transport of lithium ions and the electrochemical reactions at electrodes proceed with this LC electrolyte in the wide potential range for negative and positive electrodes of lithium-ion batteries.

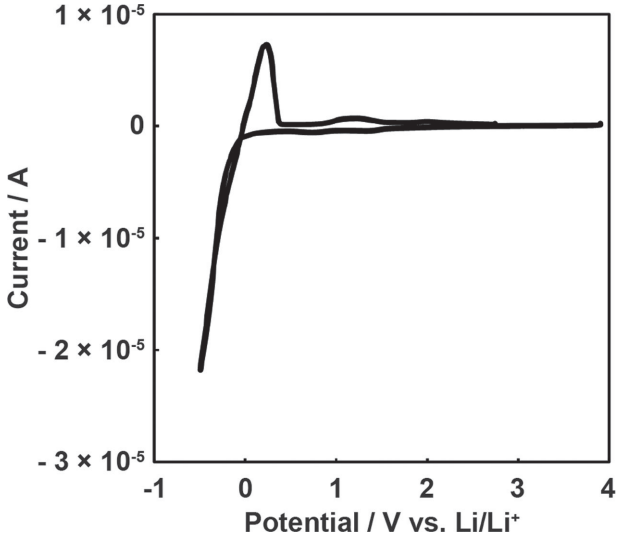

Figure 4. Cyclic voltammogram of the Li/LC electrolyte containing **1**/stainless-steel (SUS316L) cell at the scan rate of 0.025 mV s^{-1} and in the potential range from –0.5 to 3.9 V versus Li/Li^+ at 60 °C.

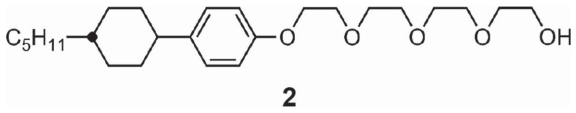

2

Figure 5. Molecular structure of compound **2**.[6c]

The achievement of the LC electrolyte with sufficient electrochemical stability appears to be owing to the employment of the cyclic carbonate group as the ion-conductive moiety and the cyclohexylphenyl mesogen. This moiety is expected to be electrochemically less reactive than conventional aromatic mesogens like biphenyls and terphenyls. We reported a rod-like molecule **2**[6c] having a tetraethylene glycol-based ion-conductive part (**Figure 5**). Compound **2** has the cyclohexylphenyl group, which is the same mesogenic moiety as that of compound **1**. For comparison, the electrochemical stability of compound **2** was studied. In cyclic voltammetry for the LC electrolyte containing **2** and LiTFSI in the 9:1 molar ratio, the anodic current deriving from the degradation of the electrolyte was observed and the decomposed product inhibited lithium deposition and dissolution on the electrode (Supporting Information, Figure S5). Electrochemical stability should be considered in the molecular design for the application of LC electrolytes to lithium-ion batteries.

2.4. Charge–Discharge of Electrodes for Lithium-Ion Batteries

In order to study the applicability of the electrolyte to lithium-ion batteries, Li/LC electrolyte/$LiFePO_4$, and Li/LC electrolyte/$Li_4Ti_5O_{12}$ coin cells were prepared and examined by galvanostatic charge–discharge experiments. $LiFePO_4$ is a positive electrode active material widely used in lithium-ion batteries, while $Li_4Ti_5O_{12}$ is used as a negative electrode.[16] The mixture of **1** and LiTFSI in the molar ratio of 9:1 was used as the LC electrolyte.

Figure 6 presents the electrochemical properties of the Li/LC electrolyte/$LiFePO_4$ cell at 60 °C. Figure 6a shows the charge–discharge curves of the cell during the initial 30 cycles in the potential range from 2.5 to 3.9 V versus Li/Li^+ at the current density of 5 mA g^{-1}. The constant potential region around 3.4 V versus Li/Li^+ was observed for the charge–discharge curves, suggesting that reversible charge–discharge reactions proceeded. The discharge capacity of the 30th cycle was 123 mA h g^{-1}, which was 92% of the initial discharge capacity. The Li/LC electrolyte/$LiFePO_4$ cell showed no significant degradation of the capacity during the cycles (Figure 6b). The electrochemical stability of the LC electrolyte in the high potential range leads to stable charge–discharge cycles.

The electrochemical properties of the Li/LC electrolyte/$Li_4Ti_5O_{12}$ cell at 60 °C are shown in **Figure 7**. Figure 7a presents the charge–discharge curves of the Li/LC electrolyte/$Li_4Ti_5O_{12}$ cell during the initial 30 cycles in the potential range from 1.2 to 3.0 V versus Li/Li^+ at the current density of 5 mA g^{-1}. This cell also showed reversible charge–discharge behavior, indicated by the constant potential region around 1.5 V versus Li/Li^+ in the charge–discharge curves. However, discharge capacity decreased during the charge–discharge cycles (Figure 7b). This decrease in the capacity

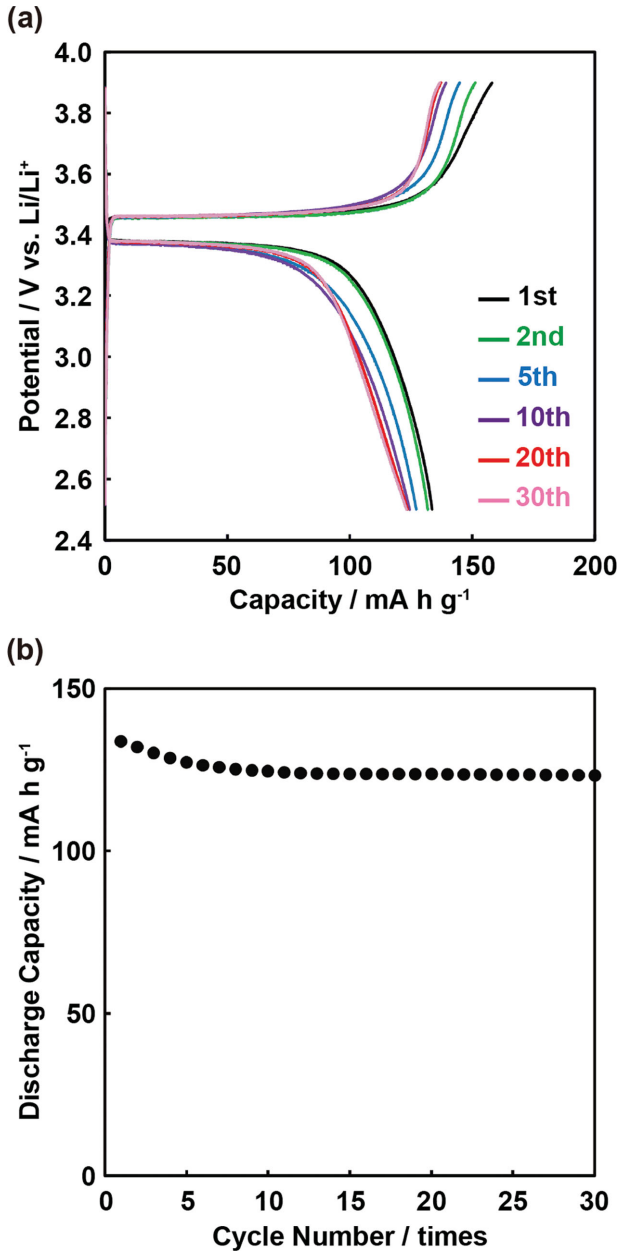

Figure 6. a) Charge–discharge curves and b) cycle performance of the Li/LC electrolyte containing **1**/$LiFePO_4$ cell at the current density of 5 mA g^{-1} at 60 °C.

can be ascribed to the partial degradation of the LC electrolyte which is gradually reduced below 1.5 V versus Li/Li^+ (Figure 4). This reduction may not give a passivating surface film desirable for the protection of the electrolyte and for the stable charge–discharge cycles.

Although the orientation of ion-conductive pathways of the nanostructured electrolytes was not controlled in the charge–discharge experiments in the present study, we expect the pathways are partially continuous at the border of polydomain. The performance of batteries could be improved if we achieved the uniform alignment of 2D pathways in the direction perpendicular to the surface of electrode materials.

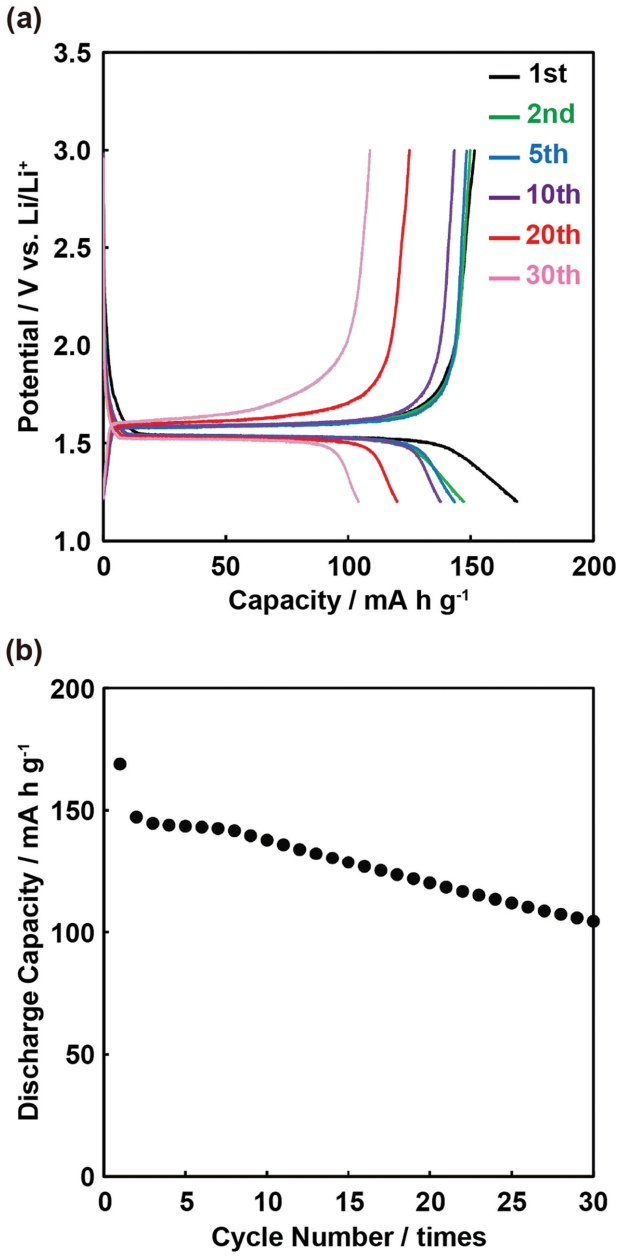

Figure 7. a) Charge–discharge curves and b) cycle performance of the Li/LC electrolyte containing **1**/$Li_4Ti_5O_{12}$ cell at the current density of 5 mA g^{-1} at 60 °C.

3. Conclusion

For the first time, we have shown that thermotropic liquid crystals can be applied as electrolytes in lithium-ion batteries. New ion-conductive LC materials composed of cyclic carbonate-based LC molecule **1** and LiTFSI have been prepared. These materials exhibit thermotropic SmA phases having 2D ion-conductive pathways in wide temperature ranges. The thermotropic LC electrolyte consisting of **1** and LiTFSI in the 9:1 molar ratio shows the sufficient electrochemical stability for use in lithium-ion batteries. The reversible charge–discharge of both $LiFePO_4$ positive electrode and $Li_4Ti_5O_{12}$ negative electrode of lithium-ion batteries has been achieved with this electrolyte in the thermotropic LC state. In terms of cycle performances and rate capabilities of the batteries, the performance of the LC electrolyte in the present study is lower than the state-of-the-art organic liquid,[12] gel,[3a,b] and solid[4] electrolytes. However, this first demonstration of the applicability of LC electrolytes to the lithium-ion battery may lead to improvement of the batteries through the continuous research on molecular design, control over LC nanostructures, and alignment of ion-conductive pathways.

4. Experimental Section

General Procedures: ^1H and ^{13}C NMR spectra were taken on a JEOL JNM-ECX400 at 400 and 100 MHz in $CDCl_3$, respectively. Chemical shifts of ^1H and ^{13}C NMR signals were quoted to Me_4Si ($\delta = 0.00$) and $CDCl_3$ ($\delta = 77.00$) as internal standards, respectively, and expressed by chemical shifts in ppm (δ), multiplicity, coupling constant (Hz), and relative intensity. FT-IR measurements were carried out with a JASCO FT/IR-6100. Matrix-assisted laser desorption ionization time-of-flight mass spectra (MALDI-TOF MS) were obtained using a Bruker Daltonics Autoflex Speed using dithranol as the matrix. Elemental analyses were conducted on an Exeter Analytical CE440 elemental analyzer. The thermal properties of the materials were examined by a differential scanning calorimetry (DSC) using a Netzsch DSC204 Phoenix. The heating and cooling rates were 10 K min^{-1}. Transition temperatures were taken at the onsets of the transition peaks on first cooling. A polarizing optical microscope Olympus BX53 equipped with a Linkam LTS350 hot stage was used to study liquid crystallinity. X-ray diffraction patterns were taken on a Rigaku RINT-2500 diffractometer with CuKα radiation. Molecular mechanics calculations were carried out with a Wavefunction SPARTAN'10 (v. 1.1.0) program.

Materials: All chemical reagents and solvents used for the synthesis of compound **1** were obtained from commercial sources and used without purification. Lithium *bis*(trifluoromethylsulfonyl)imide (LiTFSI) in a lithium battery grade was purchased from Kishida Chemical and mixed with compound **1**.

Synthesis of Compound ***1***: A diol compound, 6-[4-(*trans*-4-Pentylcyclohexyl)phenoxy]hexane-1,2-diol (**2**) was obtained according to the method previously reported.[15b] Compound **2** (2.03 g, 5.59 mmol) and a mixture of KF and Al_2O_3 (1 g) were dissolved in diethylcarbonate (40 mL). The reaction mixture was refluxed for 5 h at 140 °C. After cooling, the reaction mixture was diluted with $CHCl_3$. The precipitate of KF and Al_2O_3 were then discarded by filtration. The solvent was removed under vacuum and the crude product was purified by silica gel chromatography (eluent: hexane/$CHCl_3$ = 1:1). Further recrystallization in methanol gave compound **1** in 85% yield (1.85 g, 4.77 mmol). ^1H NMR (400 MHz, $CDCl_3$): $\delta = 7.11$ (d, $J = 8.8$ Hz, 2H), 6.80 (d, $J = 8.8$ Hz, 2H), 4.71 (m, 1H), 4.52 (t, $J = 8.0$ Hz, 1H), 4.07 (t, $J = 7.8$ Hz, 1H), 3.95 (t, $J = 6.2$ Hz, 2H), 2.40 (tt, $J = 3.0$ Hz, 12 Hz, 1H), 1.89–1.81 (m, 7H), 1.81–1.56 (m, 3H), 1.45–1.17 (m, 11H), 1.07–0.97 (m, 2H), 0.89 (t, $J = 7.0$ Hz, 3H). ^{13}C NMR (100 MHz, $CDCl_3$): $\delta = 156.99$, 155.06, 140.39, 127.76, 114.29, 76.97, 69.41, 67.29, 43.82, 37.48, 37.41, 34.68, 33.74, 33.71, 32.31, 28.89, 26.75, 22.80, 21.45, 14.21. IR (KBr): 3041, 2954, 2916, 2847, 1804, 1610, 1580, 1514, 1471, 1391, 1283, 1248, 1181, 1155, 1111, 1075, 1056, 1021, 829, 775, 737, 625, 545 cm^{-1}. MS (MALDI-TOF): calcd. for $[M + Na]^+$, 411.53; found, 411.45. Elemental analysis: calcd. (%) for $C_{24}H_{36}O_4$: C, 74.19; H, 9.34. Found: C, 74.20; H, 9.41.

Preparation of the Mixtures of ***1*** *and LiTFSI*: The mixtures of compound **1** and LiTFSI were prepared by slow evaporation of the solvent at 80 °C from tetrahydrofuran solutions containing requisite amounts of **1** and LiTFSI followed by drying under reduced pressure at 80 °C. The mixture in the 9:1 molar ratio was used as the liquid-crystalline (LC) electrolyte for electrochemical measurements.

Measurements of Ionic Conductivities: Temperature dependence of ionic conductivities was measured by the alternating current impedance method using a Solartron 1260 impedance/gain-phase analyzer (frequency range: 100 Hz–1 MHz, applied voltage: 0.6 V) equipped with a temperature controller. The cooling rates were fixed to 2 K min^{-1}. Ionic conductivities were practically calculated to be the product of $1/R_b$ (Ω^{-1}) times cell constants (cm^{-1}) for comb-shaped gold electrodes, which were calibrated with KCl aqueous solution (1.00 mmol L^{-1}) as a standard conductive solution. The impedance data were modeled as a connection of two *RC* circuits in series.

Cyclic Voltammetry: Coin-type test cells were assembled in an argon-filled glove box. A stainless-steel plate (SUS-316L) was utilized as a working electrode. A lithium metal was used as a reference and counter electrode. Separator was a polypropylene film filled with the LC electrolyte. The cyclic voltammogram was recorded on a Solartron 1470 potentiostatic-galvanostatic system within the potential range from –0.5 to 3.9 V versus Li/Li^+ at the scan rate of 0.025 mV s^{-1} at 60 °C.

Charge–Discharge Experiments: The powder of $LiFePO_4$ (SLFP-PT30, Tatung Fine Chemical) or $Li_4Ti_5O_{12}$ (LT-015, Ishihara Sangyo) was used as the active material. Carbon black (Super P-Li, TIMCAL) was used as an electrically conductive additive. Poly(vinylidene difluoride) (PVDF#1300 for $LiFePO_4$, PVDF#1100 for $Li_4Ti_5O_{12}$, Kureha) dissolved in N-methylpyrrolidinone (NMP) was used as a binder. The proportion of the materials in the electrodes was 65:35:5 by mass after drying. To prepare the suspensions, all electrode constituents were mixed in NMP with an ultrasonic homogenizer (UH-50, SMT Co., Ltd.). The $LiFePO_4$ or $Li_4Ti_5O_{12}$ electrode was prepared by spreading each slurry onto an Al-foil or a Cu-foil current collector, respectively. The circular electrodes were dried at 100 °C in a vacuum oven. Coin-type test cells were assembled in an argon-filled glove box. A lithium metal was used as a reference and counter electrode. Separator was a polypropylene film filled with the LC electrolyte. Galvanostatic charge–discharge cycling of $LiFePO_4$ or $Li_4Ti_5O_{12}$ electrode was conducted on a Hokuto Denko HJ1001SM8A galvanostat in the potential range from 2.5 to 3.9 V or from 1.2 to 3.0 V versus Li/Li^+ at the current density of 5 mA g^{-1} at 60 °C, respectively. The $LiFePO_4$ active material obtained from a commercial source contains a small amount of conductive material to improve electronic conductivity. The specific capacity and specific current were calculated with the weight of this composite.

Supporting Information

Supporting Information is available from the Wiley Online Library or from the author.

Acknowledgements

This study was partially supported by the Funding Program for World-Leading Innovative R&D on Science and Technology (FIRST) from the Cabinet Office, Government of Japan and a Grant-in-Aid for Scientific Research (No. 22107003) on Innovative areas: "Fusion Materials: Creative Development of Materials and Exploration of Their Function through Molecular Control" (Area No. 2206) from the Ministry of Education, Culture, Sports, Science and Technology. J.S. is grateful for financial support from the JSPS Research Fellowships for Young Scientists. The authors would like to thank Prof. Tetsuichi Kudo and Dr. Mitsuhiro Hibino for fruitful discussions.

Received: July 26, 2014
Revised: September 27, 2014
Published online: December, 22, 2014

[1] a) *Handbook of Liquid Crystals*, 2nd ed. (Eds: J. W. Goodby, P. J. Collings, T. Kato, C. Tschierske, H. Gleeson, P. Raynes), Wiley-VCH, Weinheim, Germany **2014**; b) J. Wu, W. Pisula, K. Müllen, *Chem. Rev.* **2007**, *107*, 718; c) S. Sergeyev, W. Pisula, Y. H. Geerts, *Chem. Soc. Rev.* **2007**, *36*, 1902; d) T. Kato, N. Mizoshita, K. Kishimoto, *Angew. Chem. Int. Ed.* **2006**, *45*, 38; e) T. Kato, *Science* **2002**, *295*, 2414; f) M. O'Neill, S. M. Kelly, *Adv. Mater.* **2011**, *23*, 566.

[2] a) R. L. Kerr, S. A. Miller, R. K. Shoemaker, B. J. Elliott, D. L. Gin, *J. Am. Chem. Soc.* **2009**, *131*, 15972; b) T. Kato, *Angew. Chem.* **2010**, *122*, 8019; *Angew. Chem Int. Ed.* **2010**, *49*, 7847; c) B. R. Wiesenauer, D. L. Gin, *Polym. J.* **2012**, *44*, 461; d) B.-K. Cho, *Polym. J.* **2012**, *44*, 475; e) Y. Zheng, J. Lui, G. Ungar, P. V. Wright, *Chem. Rec.* **2004**, *4*, 176; f) O. Ikkala, G. ten Brinke, *Chem. Commun.* **2004**, 2131; g) M. Yoshio, T. Kato, in *Handbook of Liquid Crystals*, Vol. *8, 2nd ed.* (Eds: J. W. Goodby, P. J. Collings, T. Kato, C. Tschierske, H. Gleeson, P. Raynes), Wiley-VCH, Weinheim, Germany **2014**, pp 727—749, Ch. 23.

[3] a) J. Y. Song, Y. Y. Wang, C. C. Wan, *J. Power Sources* **1999**, *77*, 183; b) A. M. Stephan, *Eur. Polym. J.* **2006**, *42*, 21; c) J. M. Pringle, P. C. Howlett, D. R. MacFarlane, M. Forsyth, *J. Mater. Chem.* **2010**, *20*, 2056; d) M. Armand, F. Endres, D. R. MacFarlane, H. Ohno, B. Scrosati, *Nat. Mater.* **2009**, *8*, 621; e) D. R. MacFarlane, J. Huang, M. Forsyth, *Nature* **1999**, *402*, 792; f) P. V. Wright, *Electrochim. Acta* **1998**, *43*, 1137; g) W. H. Meyer, *Adv. Mater.* **1998**, *10*, 439; h) F. Croce, G. B. Appetecchi, L. Persi, B. Scrosati, *Nature* **1998**, *394*, 456.

[4] a) N. Kamaya, K. Homma, Y. Yamakawa, M. Hirayama, R. Kanno, M. Yonemura, T. Kamiyama, Y. Kato, S. Hama, K. Kawamoto, A. Mitsui, *Nat. Mater.* **2011**, *10*, 682; b) T. Minami, A. Hayashi, M. Tatsumisago, *Solid State Ionics* **2006**, *177*, 2715; c) F. Mizuno, A. Hayashi, K. Tadanaga, M. Tatsumisago, *Adv. Mater.* **2005**, *17*, 918; d) P. Knauth, *Solid State Ionics* **2009**, *180*, 911.

[5] a) H. Shimura, M. Yoshio, A. Hamasaki, T. Mukai, H. Ohno, T. Kato, *Adv. Mater.* **2009**, *21*, 1591; b) M. Yoshio, T. Mukai, H. Ohno, T. Kato, *J. Am. Chem. Soc.* **2004**, *126*, 994; c) V. Percec, G. Johansson, J. Heck, G. Ungar, S. V. Batty, *J. Chem. Soc., Perkin Trans. 1* **1993**, 1411.

[6] a) T. Ohtake, K. Ito, N. Nishina, H. Kihara, H. Ohno, T. Kato, *Polym. J.* **1999**, *31*, 1155; b) K. Kishimoto, T. Suzawa, T. Yokota, T. Mukai, H. Ohno, T. Kato, *J. Am. Chem. Soc.* **2005**, *127*, 15618; c) Y. Iinuma, K. Kishimoto, Y. Sagara, M. Yoshio, T. Mukai, I. Kobayashi, H. Ohno, T. Kato, *Macromolecules* **2007**, *40*, 4874; d) G. S. McHattie, C. T. Imrie, M. D. Ingram, *Electrochim. Acta* **1998**, *43*, 1151; e) M. Yoshio, T. Mukai, K. Kanie, M. Yoshizawa, H. Ohno, T. Kato, *Chem. Lett.* **2002**, 320; f) C. J. Bowlas, D. W. Bruce, K. R. Seddon, *Chem. Commun.* **1996**, 1625.

[7] a) B.-K. Cho, A. Jain, S. M. Gruner, U. Wiesner, *Science* **2004**, *305*, 1598; b) T. Ichikawa, M. Yoshio, A. Hamasaki, T. Mukai, H. Ohno, T. Kato, *J. Am. Chem. Soc.* **2007**, *129*, 10662; c) T. Ichikawa, M. Yoshio, A. Hamasaki, S. Taguchi, F. Liu, X. Zeng, G. Ungar, H. Ohno, T. Kato, *J. Am. Chem. Soc.* **2012**, *134*, 2634.

[8] a) M. Henmi, K. Nakatsuji, T. Ichikawa, H. Tomioka, T. Sakamoto, M. Yoshio, T. Kato, *Adv. Mater.* **2012**, *24*, 2238; b) A. P. H. J. Schenning, Y. C. Gonzalez-Lemus, I. K. Shishmanova, D. J. Broer, *Liq. Cryst.* **2011**, *38*, 1627; c) C. L. Gonzalez, C. W. M. Bastiaansen, J. Lub, J. Loos, K. Lu, H. J. Wondergem, D. J. Broer, *Adv. Mater.* **2008**, *20*, 1246.

[9] a) S. Ueda, J. Kagimoto, T. Ichikawa, T. Kato, H. Ohno, *Adv. Mater.* **2011**, *23*, 3071; b) T. Ichikawa, T. Kato, H. Ohno, *J. Am. Chem. Soc.* **2012**, *134*, 11354; c) B. Soberats, M. Yoshio, T. Ichikawa, S. Taguchi, H. Ohno, T. Kato, *J. Am. Chem. Soc.* **2013**, *135*, 15286.

[10] a) N. Yamanaka, R. Kawano, W. Kubo, T. Kitamura, Y. Wada, M. Watanabe, S. Yanagida, *Chem. Commun.* **2005**, 740; b) R. D. Costa, F. Werner, X. Wang, P. Grönninger, S. Feihl, F. T. U. Kohler, P. Wasserscheid, S. Hibler, R. Beranek, K. Meyer, D. M. Guldi, *Adv. Energy Mater.* **2013**, *3*, 657.

[11] a) J. B. Goodenough, Y. Kim, *Chem. Mater.* **2010**, *22*, 587; b) M. S. Whittingham, *Chem. Rev.* **2004**, *104*, 4271; c) J.-M. Tarascon, M. Armand, *Nature* **2001**, *414*, 359; d) N.-S. Choi, Z. Chen, S. A. Freunberger, X. Ji, Y.-K. Sun, K. Amine, G. Yushin, L. F. Nazar, J. Cho, P. G. Bruce, *Angew. Chem. Int. Ed.* **2012**, *51*, 9994; e) A. Yoshino, *Angew. Chem.* **2012**, *124*, 5898; *Angew. Chem. Int. Ed.* **2012**, *51*, 5798; f) M.-R. Gao, Y.-F. Xu, J. Jiang, S.-H. Yu, *Chem. Soc. Rev.* **2013**, *42*, 2986.
[12] K. Xu, *Chem. Rev.* **2004**, *104*, 4303.
[13] a) M. Yoshio, T. Kagata, K. Hoshino, T. Mukai, H. Ohno, T. Kato, *J. Am. Chem. Soc.* **2006**, *128*, 5570; b) T. Ichikawa, M. Yoshio, A. Hamasaki, J. Kagimoto, H. Ohno, T. Kato, *J. Am. Chem. Soc.* **2011**, *133*, 2163; c) K. Kishimoto, M. Yoshio, T. Mukai, M. Yoshizawa, H. Ohno, T. Kato, *J. Am. Chem. Soc.* **2003**, *125*, 3196; d) K. Hoshino, M. Yoshio, T. Mukai, K. Kishimoto, H. Ohno, T. Kato, *J. Polym. Sci., Part A: Polym. Chem.* **2003**, *41*, 3486; e) A. Yamashita, M. Yoshio, S. Shimizu, T. Ichikawa, H. Ohno, T. Kato, *J. Polym. Sci., Part A: Polym. Chem.,* DOI: 10.1002/pola.27380.
[14] S. Bhattacharya, S. V. Letcher, *Phys. Rev. Lett.* **1979**, *42*, 458.
[15] a) M. Yoshio, T. Mukai, K. Kanie, M. Yoshizawa, H. Ohno, T. Kato, *Adv. Mater.* **2002**, *14*, 351; b) M. Yoshio, T. Kato, T. Mukai, M. Yoshizawa, H. Ohno, *Mol. Cryst. Liq. Cryst.* **2004**, *413*, 2235.
[16] a) L.-X. Yuan, Z.-H. Wang, W.-X. Zhang, X.-L. Hu, J.-T. Chen, Y.-H. Huang, J. B. Goodenough, *Energy Environ. Sci.* **2011**, *4*, 269; b) G.-N. Zhu, Y.-G. Wang, Y.-Y. Xia, *Energy Environ. Sci.* **2012**, *5*, 6652.